

R. CESTER, etc.
1958, Febbraio
Il Nuovo Cimento
Serie X, Vol. 7, pag. 371-399

On the Charge and Energy Spectrum of Heavy Primaries in Cosmic Radiation.

R. CESTER, A. DEBENEDETTI, C. M. GARELLI, B. QUASSIATI,
L. TALLONE and M. VIGONE

Istituto di Fisica dell'Università - Torino
Istituto Nazionale di Fisica Nucleare - Sezione di Torino

(ricevuto il 1º Novembre 1957)

Summary. — 529 tracks of heavy primaries in the cosmic radiation have been studied. Charge measurements have been carried out on all tracks with a photometric method, and independent checks with gap counting have been performed on Boron and Carbon tracks. All tracks have been followed through and a total of 331 nuclear collisions observed. From the analysis of these interactions, the interaction mean free paths and fragmentation probabilities in emulsion and in air have been determined. The results are in good agreement with those of other workers and have been used to extrapolate the charge distribution at the top of the atmosphere: the ratios of light nuclei and of heavy nuclei to medium nuclei, at the top of the atmosphere, are 0.30 ± 0.09 and 0.51 ± 0.11 respectively. Results of energy determination on 275 tracks give a value $1.54^{+0.16}_{-0.13}$ for the exponent of the integral energy spectrum. Some difficulties in the application of Peters' relation between the energy of primary and the angles of emission of the fragmentation products are discussed.

1. - Introduction.

The knowledge of the relative abundance of the heavy primaries and of their energy spectrum is very important in order to study the origin of the cosmic radiation. Experimental data on this subject have been given by many

authors (¹⁻⁸), but the results are not in perfect agreement. This discrepancy is probably due to the difficulty of avoiding systematic errors and of having a large statistics.

The present work will add some experimental results to the ones that have already been collected. In order to reduce the uncertainty due to possible errors in the measurements, we divided the charge spectrum in three groups: L group ($3 \leq Z \leq 5$); M group ($6 \leq Z \leq 9$); H group ($Z \geq 10$). We discuss carefully all the types of measurements made, and we try to check the results with independent methods every time it is possible.

2. - Exposure details.

Two stacks flown at high altitude at the same latitude were used in this work. One, which we shall indicate as Y-stack, was a stack of 38 stripped Ilford G5 emulsions ($38 \text{ cm} \times 25 \text{ cm} \times 0.06 \text{ cm}$). It was exposed with vertical orientation of the 38 cm side, over Northern Italy ($\lambda = 46^\circ \text{ N}$) at an atmospheric depth of about 15 g/cm^2 . To the amount of atmosphere above the stack must be added the thickness of the packing material which was 2 g/cm^2 . The other stack, indicated as B-stack, of 70 stripped $15 \text{ cm} \times 15 \text{ cm} \times 0.06 \text{ cm}$ Ilford G5 emulsions, was flown at the same latitude of 46° N , under a depth of 12 g/cm^2 of air and packing material.

3. - Detection of particles.

All plates of the Y-stack were scanned along a line parallel to and 3 mm below the upper edge, for tracks satisfying the following criteria:

- 1) Projected length $> 2 \text{ mm/plate}$.
- 2) Grain density greater than about nine times the minimum value.

The total area scanned in this way was 55 cm^2 .

The scanning of the B-stack was made, under the same criteria, on all

(¹) H. L. BRADT and B. PETERS: *Phys. Rev.*, **80**, 943 (1950).

(²) A. D. DAINTON, P. H. FOWLER and D. W. KENT: *Phil. Mag.*, **43**, 729 (1952).

(³) M. F. KAPLON, B. PETERS, H. L. REYNOLDS and D. M. RITSON: *Phys. Rev.*, **85**, 295 (1952).

(⁴) K. GOTTSSTEIN: *Phil. Mag.*, **45**, 347 (1954).

(⁵) M. F. KAPLON, J. H. NOON and G. W. RACETTE: *Phys. Rev.*, **96**, 1408 (1954).

(⁶) J. H. NOON and M. F. KAPLON: *Phys. Rev.*, **97**, 769 (1955).

(⁷) H. FAY: *Zeits. f. Naturf.*, **10a**, 572 (1955).

(⁸) J. H. NOON, A. J. HERTZ and B. J. O'BRIEN: *Nuovo Cimento*, **5**, 854 (1957).

plates of the stack along a 5 cm long line, 1 cm below the top edge of the emulsions (total area scanned 21 cm²). The total depth under which the scanning of the B-stack was performed was about 16 g/cm² (3.8 g/cm² of emulsion and 12 g/cm² of air and packing material).

Only the tracks that had a projected length $l \geq 3$ mm/plate were considered in this work. They were followed through the stack until they left or interacted; if a heavy fragment emerged from an interaction, this fragment was also followed.

A special scanning for Li and Be tracks was made in the Y-stack on an area of 23 cm² and all tracks of $I/I_0 > 7$ were detected. In order to distinguish the Li-tracks from the background of singly charged and α -particles, all tracks of $I/I_0 > 7$ were followed through a range ≥ 5 cm and those stopping or showing a change in ionization were rejected. The remaining tracks were accepted for measurements and followed through the whole stack. We believe that no Li and Be tracks in the area re-scanned in this way could be missed.

No special scanning for Li and Be tracks was made in the B-stack.

On the whole a total of 529 tracks (415 in the Y-stack and 114 in the B-stack) of particles ranging from Li to Fe were detected and studied in this work.

4. - Charge measurements.

Since the cut-off energy for 46° N latitude has been shown to be 1.55 GeV per nucleon (⁹), nearly all the primary heavy nuclei which entered the stack were relativistic and charge can be determined without ambiguity from ionization.

4.1. Photometric measurements. – Charge determinations were made on all tracks with a photoelectric device that has been previously described (¹⁰). Details on these measurements will be given elsewhere (¹¹). The photometric absorption of all tracks was determined at the same depth below the emulsion surface. As the results are sensitive to the dip of the track, the plates were inclined so that the section of the track that was measured was adjusted nearly parallel to the photomultiplier slit. In order to reduce the effect of background and of local fluctuations in the development, a total length of 3 000 μ m of each track was measured, the measurements being performed (whenever possible)

(⁹) P. H. FOWLER and C. J. WADDINGTON: *Phil. Mag.*, **1**, 637 (1957).

(¹⁰) M. ARTOM and C. GENTILE: *Suppl. Nuovo Cimento*, **4**, 254 (1956).

(¹¹) M. ARTOM, V. BISI and C. GENTILE: *Ric. Scient.*, (1957) (in the press).

in four different emulsion sheets. On some of the tracks a total length shorter than 3 mm was available, or measurements could be performed only in one or two different emulsion sheets. In these cases gap or δ -rays counting was carried on.

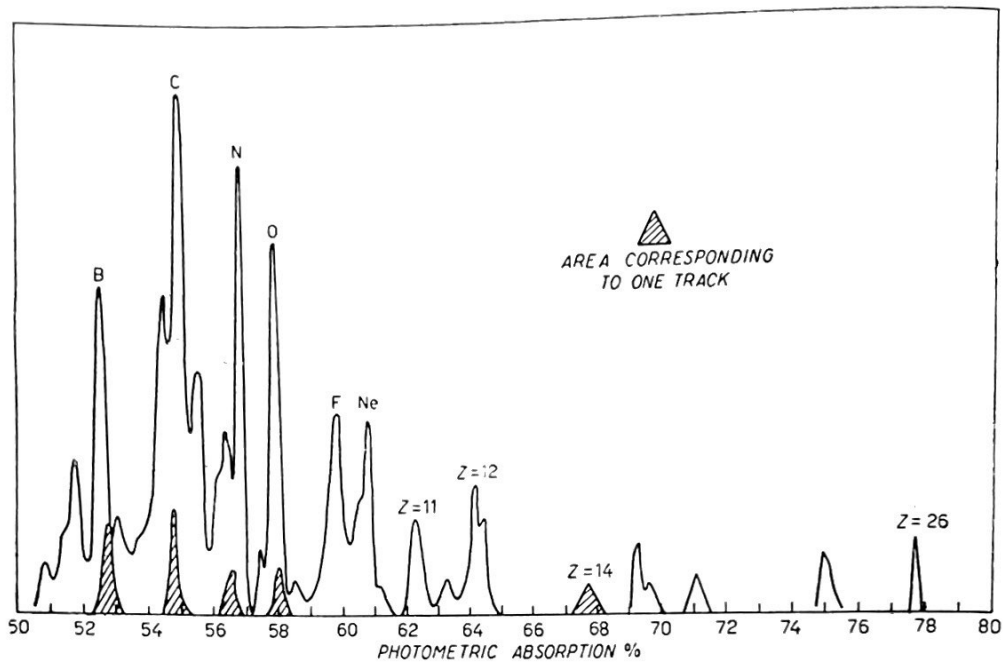


Fig. 1.

The results of the photometric measurements are shown in the two histograms of Fig. 1 and Fig. 2 in which each track is represented as a triangle of

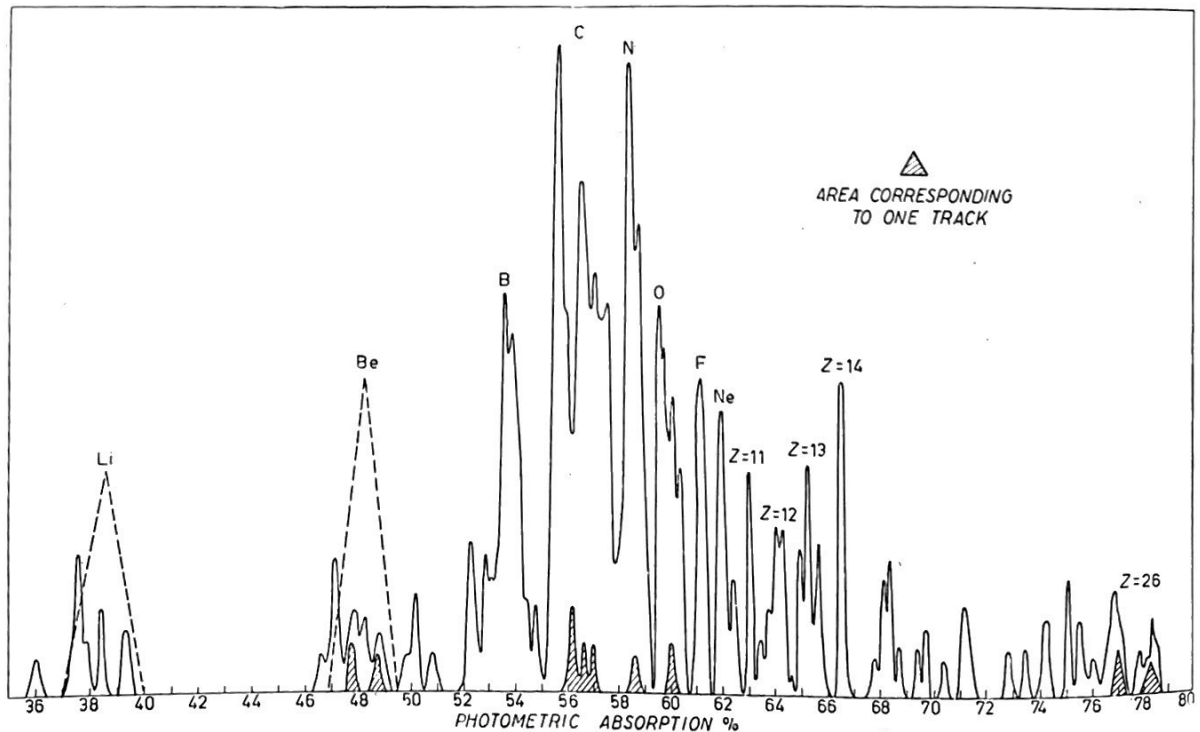


Fig. 2.

constant area with a base equal to twice the standard deviation. The resolution is better in the histogram of the B-stack (Fig. 1) owing to the very good development of this stack. In this histogram however we do not report the Li and Be tracks as in the B-stack no special scanning for these tracks was carried out and the scanning efficiency in this charge interval was not very good.

In Fig. 2 the area under the dashed curve represents the number of Li and Be particles increased by the corresponding loss correction factors that take into account the results of the special scanning.

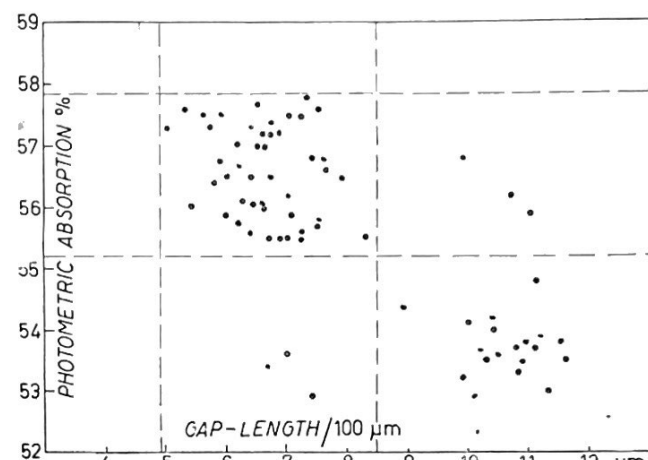


Fig. 3.

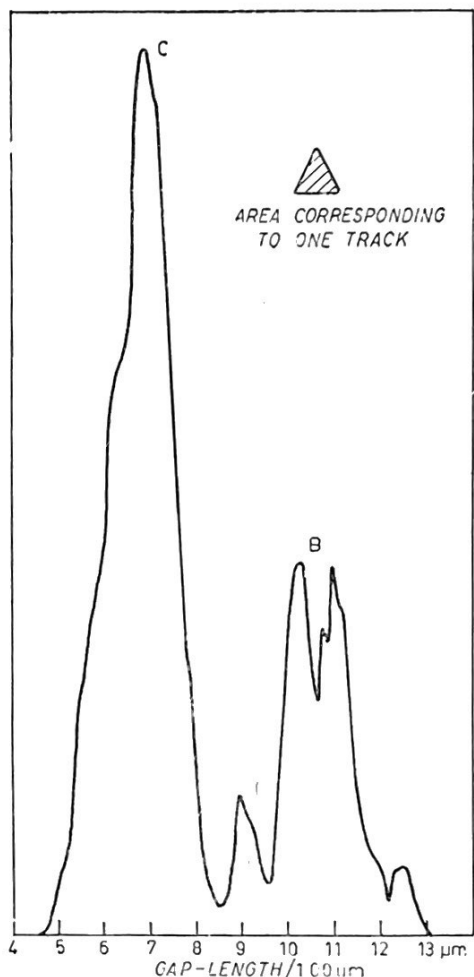


Fig. 4.

Charge calibration has been made on the splitting tracks whose charge could be unambiguously determined from the products of fragmentation. The corresponding interactions are indicated by a star in Table III-a and III-b of Sect. 6 and the corresponding area is dashed in the histograms. These tracks were also used to obtain the calibration for δ -rays and gap-length measurements.

The identification of charges is reliable up to about $Z = 14$; for greater atomic number, owing to low statistics and lack of calibration tracks, the determination of charge is more uncertain.

4.2. Gap length measurements. — In order to have a further check on the charge determination and to improve the resolution between Boron and Carbon, gap length measurements were carried out on all the Boron and Carbon tracks (in the Y-stack) which made an angle $\leq 30^\circ$ with the vertical. For each track a total of about $300 \div 400$ gaps, corresponding to a total track length of $3000 \mu\text{m}$, in at least three different

emulsion sheets was measured. The gap length obtained (length of gaps per 100 μm of track) are plotted against the photometric absorption in Fig. 3 which shows a good agreement between the two types of measurements. Of the total of 65 particles, 58 have the same charge in both determinations, while for 8 tracks the two methods give two values of Z differing by one.

In Fig. 4 the results of gap length measurements are shown in the form of an histogram.

5. - Scanning efficiency.

To check the scanning efficiency we determined for the Y-stack the distribution in length per plate of the particles. We divided the tracks in the following three groups of dip angles ξ : $6^{\circ}50' \leq \xi < 11^{\circ}$; $3^{\circ}30' \leq \xi < 6^{\circ}50'$; and $0^{\circ} \leq \xi < 3^{\circ}30'$; corresponding to lengths per plate l of $3 \div 5 \text{ mm}$, $5 \div 10 \text{ mm}$, $> 10 \text{ mm}$ respectively. If the efficiency of detection is the same for all plates, the number n of tracks per plate and per unit solid angle (*) must be practically the same for all groups. A certain loss for very flat tracks and for the shorter ones is evident from the results of Table I.

TABLE I. – Number of tracks per plate and per steradian.

	$3 \text{ mm} \leq \frac{\text{length}}{\text{plate}} < 5 \text{ mm}$	$5 \text{ mm} \leq \frac{\text{length}}{\text{plate}} < 10 \text{ mm}$	$\frac{\text{length}}{\text{plate}} \geq 10 \text{ mm}$	$\frac{\text{length}}{\text{plate}} \geq 3 \text{ mm}$
All observers	4.4 ± 0.2	5.6 ± 0.3	3.6 ± 0.3	4.5 ± 0.2
Good observers	4.8 ± 0.3	5.9 ± 0.4	3.8 ± 0.3	4.8 ± 0.2

We also compared the values of n for the various scanners and they turned out to be the same for all but one. We can try to evaluate a correction factor for scanning loss, dividing the value of n for good observers and for l ranging from 5 mm to 10 mm, by the value of n for all tracks and for all observers. This correction factor turns out to be $5.9/4.5 = 1.3$.

(*) The solid angle corresponding to each interval $\Delta\xi = \xi_1 - \xi_2$ has been evaluated, and for small values of ξ is simply related to ξ_1 and ξ_2 :

$$\Delta\Omega \cong 2\pi(\cos \xi_1 - \cos \xi_2) + 4\left(\xi_2 - \frac{\pi}{2}\right)\sin \xi_2 - 4\left(\xi_1 - \frac{\pi}{2}\right)\sin \xi_1.$$

It is anyhow important to note that the relative abundances of light, medium and heavy nuclei do not vary, within statistical errors, with the angle of dip, as it is shown in Table II.

TABLE II. – *Scanning efficiency with regard to the relative abundance.*

	$3 \text{ mm} < \frac{\text{length}}{\text{plate}} < 5 \text{ mm}$	$5 \text{ mm} < \frac{\text{length}}{\text{plate}} < 10 \text{ mm}$	$\frac{\text{length}}{\text{plate}} > 10 \text{ mm}$	$\frac{\text{length}}{\text{plate}} > 3 \text{ mm}$
N_L/N_M	0.59 ± 0.08	0.53 ± 0.08	0.61 ± 0.10	all observers 0.55 good » 0.56
N_H/N_M	0.43 ± 0.09	0.29 ± 0.05	0.31 ± 0.10	all observers 0.34 good » 0.34

So that it seems reasonable to assume that the missing of tracks does not affect the determination of charge distribution. The scanning loss has to be taken into account, of course, in the evaluation of the total flux of particles entering the stack.

6. - Nuclear interactions.

331 primary and secondary interactions of heavy nuclei ($Z \geq 3$) were found on a total track length of 4660 cm traced through the Y and B-stacks. The details of each interaction are reported in Table III-a (Y-stack) and in Table III-b (B-stack).

All interactions were divided in two groups called respectively « splittings » and « stars ».

We indicate by splitting every interaction where in the direction of the primary or very close to it (within 9°) one can see:

- a) one or more tracks of fast nuclei of $Z \geq 2$ with or without relativistic tracks;
- b) a group of minimum tracks sharply divided from the other tracks of the star.

The total charge of the secondary tracks which we call splitting tracks must be compatible with the measured charge of the primary.

We call star every interaction were it is not possible to distinguish a group of fast particles in a narrow cone.

TABLE IIIa. — Characteristics of each of the 265 nuclear interactions found in the Y_{stack}
 α -particles in the splitting; p = number of protons in the splitting; $r = \frac{t_0}{t_{0[\alpha]}}$

Li					Be					B					C					
f	α	p	r	N_h	f	α	p	r	N_h	f	α	p	r	N_h	f	α	p	r	N_h	
Li	1	1			2				4*	1	3	2	3		2	2	2	2	4	
	1	1	2	3	1	2			5	2	1			3	2	2	2			
	1	1			1	2				1	3	8	3		3					
	3			6	1	2	5			1	3		2		3			1	1*	
	1	1		5	2		1		*	2	1	?			2	2	2	2	2	
		?		6	1	2				2	1	1	4		1	4	2	3	5	
	3	?		13	1	2	3		5	2	1	1	4		2	2	2	1	5	
	3			12	1	2				4		7			1	4	8	2		
	3	2		31	2		4		4	5	17	19		Li	3	5	5	3		
	?	?	?	?	1	2	?		2	2	1	3	7		2	2	2	1		
Be					2	4	15			1	3	3	2		1	4	6	5	8	
					4	5	19			2	5	7	3		6	7	6	14	1	
					1		19			B		5	1		2	5	5	3	3	
					?	?	2			Be		1	4		1	4	6	14	1	
					1	?	10					1	3	2	Li	3	5	5		
										B		1	3	4	19	2	2	4		
												5	4	9		1	4	11	15	
												1	3	16	3	C	2	4	1	
												2	1		C		3	4		
												2	1							
B												5	7	13			6	2	18	
												5	5	14		6	3	23		
												5	14	17		6	12	17		
												5	5	8		6	2	18		
												5	2	7		6	9	1		
												5	3	15		6	4	4		
												1	3	24		1	8	4		
												1	3	10	14	6	3	2		
												5	8	18		6	4	4		
												5	1	4		6	4	14		
C												5	5	14		6	4	24		
												5	12	19		6	4	4		
												5	7	7	19	1	5	5		
												5	?	6		6	6	17	18	
																3		?		

Each interaction is classified in terms of: f = number of heavy fragments; α = number of number of relativistic tracks minus p ; N_h = number of black and grey tracks.

C					N					O					F				
f	α	p	r	N_h	f	α	p	r	N_h	f	α	p	r	N_h	f	α	p	r	N_h
Be	1	6	2	1	*	1	5	1	1	4	4	2	4	*	1	7	30	?	
Be	1	6			1	5	1	3	3	4	2	2	11	Li	6	4		4	
Be	3	2	2	1	4*	Be	1	1	*	1	6			N	1				
B	2	2	2	1		B	1	7	9	15	B	3	2	5	C	9	12	4	
B	1	4	2	1			1	5	3	5	N	1	4	2	F	3	4	4	
B	2	2	*				1	5	3	9		1	4	2	O		2	2	
C	6	3	4				1	5	3	9		1	4	3	C	1	9	16	
Li	1	1	2	3		Be	1	3	5	3		1	6	3	N	1	1	2	2
Li	1	1	2	3			1	4		8		2	4	3	N	2			7
Li	3					B	2	4	4			8	5	1	Be	5	5	12	
Li	3	2	4				3	1			C	1							
B	1	5	1			B	1					8	7	16		9	7	20	
B	1	4	4	3			1	7	8	3	Be	4	7	4		9	9	21	
B	6	3	6			C	1		1	8	Li	1	3	6		8		10	
B	6	27	20				1	5		8		2	4	1		1	7	1	11
{ Li						N			3	5		3	2	3					
Li	3		1	1		N			3		C	2	?						
Li	3	2	8			Li	4	4	12	B		3	6	6					
Li	3	1	5				1	5	6	16	B	1	1	5					
Be	2	6	8			C	1	1	2	7	B	8							
C			2				1	5	6	16	N	1							
						Li	1	2	10	13									
	6	60	2									8	15	10					
	6	18	20				7	29	14			8	27	18					
	6	8	13				3		13			1	6	9	16				
	6	9	24				1	5	4	9		1	6	10	10				
	6	10	12				1	5	26	4		8	15	16					
2	2	1	3				7			9									
	6	8	11																
?	?	?	2																
?	?	?	?																
	6	11	12																
	6	4	1																
1	2		8																
?	?	?	>10																

TABLE IIIa (*continued*).

Ne					Na					Mg					Al				
f	α	p	r	N_h	f	α	p	r	N_h	f	α	p	r	N_h	f	α	p	r	
C	2					2	7	4	8	C	1	4		5		1	11		
{ Li		4	6	3	C	1	3	2				12	18	31		1	11		
Li		10	10	19	O	1	1					12	10	9	Na	1	11	3	
	2	6		4	F	1				Li	1	7	8	16	2	9	10	13	
O	1		2		Na			2	5	{ Be	1	3			3	7		1	
	1	8	36	21						Li									
Ne				1							12	70	>10			13	38	21	
Ne				1							12	13	10						
		10	6	22							1	10	19	12					
		10	34	26															
A					K					Ca					Ti				
f	α	p	r	N_h	f	α	p	r	N_h	f	α	p	r	N_h	f	α	p	r	
{ B					Si	2	1	2	4	Si	2	2	2	3		1	20	5	2
Li	1	8	16	17															
A				4							2	16	15	3					
											4	12	2						

In the first part of Tables III-a and III-b the 242 splitting events, which were studied carefully, are collected. The available information relative to the 89 stars is reported in the second part of Tables IIIa and III-b.

7. - Interaction mean free paths.

The mean free paths λ_i where $i = L, M, H$) in emulsion obtained in the Y- stack are reported in Table IV.

This result must be considered as an upper limit since we did not take into account those events in which one evaporation track only is noticed and no change of charge is detected in the incoming nucleus. Such events, as

Si					Ph					S					Cl				
<i>f</i>	α	<i>p</i>	<i>r</i>	<i>N_h</i>	<i>f</i>	α	<i>p</i>	<i>r</i>	<i>N_h</i>	<i>f</i>	α	<i>p</i>	<i>r</i>	<i>N_h</i>	<i>f</i>	α	<i>p</i>	<i>r</i>	<i>N_h</i>
O		6	1		Al	1		4	5	Ne		6	1	5	Ne		7	2	2
Na	1	1			3	9	4			N	2	5		6	Na	1	4	9	16
	1	12	3	3											B		12	26	5
	1	12	9				15	2	18									23	
		14	4	13															
		14	66	13															
		14		12															

Cr					Mn					Fe				
<i>f</i>	α	<i>p</i>	<i>r</i>	<i>N_h</i>	<i>f</i>	α	<i>p</i>	<i>r</i>	<i>N_h</i>	<i>f</i>	α	<i>p</i>	<i>r</i>	<i>N_h</i>
Sc	1	1	2	1	Cl	2	4			Mg	3	8	11	23*
S		8	16	3	Ti	1	1			Be	5	12	10	4*
N	3	11									1	24	7	8
Ph	3	3		3								26	5	13

some author pointed out (12), could in fact be due to a physical process somewhat different from the collision processes.

Our results for L and M incoming nuclei agree with those found by other authors (6, 12, 13) and with the values calculated by using for an estimate of the cross-section the empirical expression given by BRADT and PETERS (14):

$$(1) \quad \sigma_i = \pi(R_i + R_t - 2\Delta R)^2, \quad R = r_0 A^{\frac{1}{3}} \quad (r_0 = 1.45 \cdot 10^{-13} \text{ cm}),$$

(12) P. H. FOWLER, R. R. HILLIER and C. J. WADDINGTON: *Phil. Mag.*, **2**, 293 (1957).

(13) V. Y. RAJOPADHYE and C. J. WADDINGTON: Private communication.

(14) H. L. BRADT and B. PETERS: *Phys. Rev.*, **77**, 54 (1950).

TABLE III b. — Characteristics of each of the 66 nuclear interactions found in the B_{stage}
 α -particles in the splitting; p = number of protons in the splitting; $r = r_{\text{total}}$

Be					B					C					N				
f	α	p	r	N_h	f	α	p	r	N_h	f	α	p	r	N_h	f	α	p	r	N_h
Li	2	4		6		2	1		*		3			*	Be		3	3	
				1		1	3	2	6		6	4		21		1	5	2	5
	1	2	10	12		2	1	6	1		2	2		1*	C		1		5
		1	3			2	1	1			6	4		3			7	7	13
	5	2		7		2	1		1*	C			2	7	B		2	2	2
						2	1				6			16		3	1	2	1
	B						2	1	1		6	19		20	B		2	1	1
							1	3	7	18	6				Be	1	1	1	4
											2	2	1	6		2	3		2*
											6	19		1					
											2	2	4	5					
											2	2	4	17					
											2	2	4	3					
											Li	1	1		3				
											3			5					
											1	4		2					
											1	4	1	3					
												6	13	19					
												6	38	19					
												6	18	38					
												6	17	24					
												6	10	19					

where R_i is the radius of the incoming nucleus, R_t is the radius of the target nucleus and ΔR has the empirical value of $0.86 \cdot 10^{-13}$ cm. Experiments (15,16) of different kind have proved this expression to be applicable over a large range of target and incident nuclei, including the type of nuclei we are dealing with. An exception must be made for the process in which hydrogen nuclei are interested. In this case the experimental value of the σ found by CHEN and co-workers (17) by exposing a heavy nucleus target to a 860 MeV proton beam was used.

The mean free path for heavy incident nuclei found in this work is larger than the experimental and calculated values we are comparing with. This could be explained with the loss of some interactions and the only events

(15) Y. EISENBERG: *Phys. Rev.*, **96**, 1378 (1954).

(16) F. B. McDONALD: *Phys. Rev.*, **104**, 1725 (1956).

(17) F. F. CHEN, C. P. LEAVITT and A. M. SHAPIRO: *Phys. Rev.*, **99**, 857 (1955).

Each interaction is classified in terms of: f = number of heavy fragments; α = number of relativistic tracks minus p ; N_h = number of black and grey tracks.

O					F					Ne					Na					
f	α	p	r	N_h	f	α	p	r	N_h	f	α	p	r	N_h	f	α	p	r	N	
C	2	4	22	4	N			2	1	2	Be	1	4	12	11		3	5	5	
	2	2	5		N	1				O	1			2	N	4	10	16		
	1		1*		N	1								B	2	3	1	11		
	8	10	18											10	9	16				
	8	14	3											10	6	19	11	69	31	

Mg					Si					Cl					Ca				
f	α	p	r	N_h	f	α	p	r	N_h	f	α	p	r	N_h	f	α	p	r	N_h
N		5	3		C	2	4		7*	Mg	2	1	1	1	F	4	3	3	8
		12	2	31															
		12	43	36															

TABLE IV. – Mean free paths in emulsion and in air.

Charge group	λ (g/cm ²) emulsion Turin (Y-stack)	λ (g/cm ²) emulsion Bristol	λ (g/cm ²) emulsion Rochester	λ (g/cm ²) emulsion calculated value	λ (g/cm ²) air calculated value
L	60.0 ± 5.7	51.6 ± 6.1	61.7 ± 19.4	60.1	33.6
M	51.6 ± 3.3	51.9 ± 3.8	59.6 ± 6.0	49.7	26.9
H	42.5 ± 4.1	37.0 ± 3.1	36.5 ± 4.8	35.2	19.0

which we feel could be missed are those in which one or two relativistic particles only are emitted. If this is so, on the other side, we should notice also a

discrepancy between our value of the fragmentation probabilities of H nuclei in H secondaries and those found by other authors, which is not the case. We conclude then that such a high value of λ_{H} must be due to a statistical fluctuation.

In Table IV the values calculated from formula (1) of the mean free paths in air, to be used in the extrapolation of the charge spectrum to the top of the atmosphere, are also reported.

8. - Fragmentation probabilities.

In Table V are reported the fragmentation probabilities in emulsion obtained by analysing the interactions found in the Y and B-stacks. Our results are in good agreement with those of the Bristol group (12,13), while there appears to be a discrepancy between our values of P_{HL} , P_{ML} and those found by the Rochester group (6).

TABLE V. – *Fragmentation probabilities in emulsion.*

	P_{LL}	P_{ML}	P_{MM}	P_{HL}	P_{HM}	P_{HH}
Turin	0.11 ± 0.04	0.18 ± 0.03	0.16 ± 0.03	0.13 ± 0.04	0.18 ± 0.05	0.25 ± 0.06
Bristol	0.10 ± 0.04	0.12 ± 0.03	0.11 ± 0.03	0.11 ± 0.04	0.25 ± 0.06	0.16 ± 0.04
Rochester	—	0.32 ± 0.05	0.08 ± 0.03	0.43 ± 0.07	0.21 ± 0.05	0.18 ± 0.05

In order to estimate the fragmentation probabilities in air to be used for the extrapolation of the charge spectrum to the top of the atmosphere we have taken into account only those events in which $N_h \leq 7$ (*l*-events) neglecting the ones with $N_h > 7$ (*h*-events). The *l*-events are found to be 58.5% of the total number of interactions. From the emulsion composition and from the evaluation of the cross-section in emulsion, the percentage of collisions with a light target (H, C, O, N) is estimated to be 33.3%. This means that 43% of *l*-events are peripheral collisions with a heavy target. In order to estimate the fragmentation probabilities in air, we have assumed that peripheral collisions with a heavy target are felt by the incident nucleus as collisions with a light target, and therefore, we have taken as fragmentation probabilities in air those obtained by analysing *l*-events in emulsion. Our data compare with those obtained making the same assumption by the Bristol group and, since the experimental conditions and the criteria in selecting the

heavy nuclei tracks are very similar, we have used for the extrapolation to the top of the atmosphere the values obtained averaging over the results of the Turin and Bristol groups (Table VI).

TABLE VI. - *Fragmentation probabilities in l-events.*

	P_{LL}	P_{ML}	P_{MM}	P_{HL}	P_{HM}	P_{HH}
Turin	$\frac{7}{48} = 0.15$	$\frac{27}{119} = 0.23$	$\frac{23}{119} = 0.19$	$\frac{6}{44} = 0.14$	$\frac{12}{44} = 0.27$	$\frac{15}{44} = 0.34$
Bristol	$\frac{5}{31} = 0.16$	$\frac{18}{100} = 0.18$	$\frac{16}{100} = 0.16$	$\frac{5}{42} = 0.12$	$\frac{19}{42} = 0.45$	$\frac{12}{42} = 0.29$
Turin and Bristol (averaged values)	0.15 ± 0.03	0.21 ± 0.02	0.18 ± 0.02	0.13 ± 0.03	0.36 ± 0.04	0.31 ± 0.04

It must be added that the impact parameter may play an important role, as regards the fragmentation, the fragmentation being increased when the parameter decreases. In this case the previous assumption would result in an overestimate of the P_{HH} , P_{MM} , P_{LL} and in an underestimate of the P_{HL} , P_{ML} , $P_{M\alpha}$, $P_{L\alpha}$.

We did not attempt to extrapolate the charge spectrum from the top of the atmosphere to the cosmic rays origin since fragmentation probabilities of heavy primaries in hydrogen would be needed. We have reported in Table XVI (*a, b*) (Appendix II) the interactions with a proton target in emulsion but we feel that their number is much too low to give a satisfactory indication of the fragmentation probabilities in hydrogen.

9. - Charge spectrum.

The results obtained, in the Y-stack only, by measuring the heavy nuclei tracks with zenith angle $\leq 60^\circ$ were taken into account in order to determine the charge spectrum. The number of particles of each charge entering the stack at flight altitude are given in Table VII.

In the extrapolation of the charge spectrum to the top of the atmosphere we have taken in consideration only the tracks with zenith angle $\leq 30^\circ$. In this case the path in air for heavy nuclei is practically the same for all zenith angles, with a maximum spread of 8%, and therefore the computation is more

TABLE VII. – *Numbers of particles at flight altitude with zenith angle $\leq 60^\circ$.*

	Li	Be	B	C	N	O	F	$Z \geq 10$
Number of particles N_z	27	37	52	110	43	35	19	74
Relative frequencies $\frac{N_z}{\text{Total number}}$	0.07	0.09	0.13	0.27	0.11	0.09	0.05	0.18
	± 0.01	± 0.01	± 0.01	± 0.02	± 0.01	± 0.01	± 0.01	± 0.02

straightforward. Moreover, as already mentioned, we have divided all tracks in three intervals of charge, L, M, H, where: the L group includes Li, Be, B ($3 \leq Z \leq 5$); the M group includes C, N, O, F ($6 \leq Z \leq 9$); the H group includes all elements with charge $Z \geq 10$.

We used the diffusion equation reported by KAPLON *et al.* (5) and the fragmentation probabilities and mean free paths discussed in Sect. 8 and 7 and quoted in Tables VI and IV. In Table VIII the relative abundances of the three groups are given, both at flight altitude and at the top of the atmosphere.

TABLE VIII. – *Relative abundances of light, medium and heavy particles with zenith angle $\leq 30^\circ$.*

	N_L	N_M	N_H	N_L/N_M	N_H/N_M
Flight altitude	60 ± 6	130 ± 8	52 ± 5	0.46 ± 0.07	0.40 ± 0.07
Top of the atmosphere	58 ± 12	193 ± 15	99 ± 15	0.30 ± 0.09	0.51 ± 0.11

We quote the statistical errors on the number of tracks for the values at flight altitude; the errors computed for the results at the top of the atmosphere take into account statistical errors on the fragmentation probabilities as well.

To obtain the fluxes of the various components of the cosmic radiation at the top of the atmosphere, we must take in consideration the loss in the detection of particles, which was found in Sect. 5 not to be negligible. The flux for each charge component will be given by:

$$\Phi' = \frac{N^0 K}{\Delta t \cdot \Delta \Omega \cdot A} \frac{\int_0^{\theta_{\max}} \sec \theta d\theta}{\int_0^{\theta_{\max}} d\theta},$$

where N^0 is the total number of particles belonging to that charge group, A the receiving area, Δt the duration of exposure, $\Delta\Omega$ the allowed solid angle, K the correction loss factor. If we take for K the value $K=1.3$ which results from the analysis of Sect. 5, we obtain for the three components the flux values:

$$\Phi_{L^0} = 1.67 \pm 0.39 \text{ particles/m}^2 \text{ sterad s}$$

$$\Phi_{M^0} = 5.52 \pm 0.40 \quad \gg \quad \gg$$

$$\Phi_{H^0} = 2.82 \pm 0.40 \quad \gg \quad \gg$$

that are not inconsistent with the values of previous experiments.

10. - Zenith angle dependence.

The dependence of the flux of particles from the thickness of air traversed would give a check of the calculated values of the mean free paths and fragmentation probabilities in air. Therefore we studied the dependence of the heavy nuclei flux from the zenith angle θ . The weak point of this method is that, since the number of tracks decreases very rapidly with increasing zenith angles, the values corresponding to a long path of air traversed are affected by a large statistical error. In Fig. 5 the experimental quantity

$$\frac{\Delta N(\theta)}{\Delta\Omega \cos \theta}$$

(which is proportional to the flux of particles arriving at flight altitude in the solid angle $\Delta\Omega(\theta)$ (*) in a direction between θ and $\theta+\Delta\theta$) is plotted for the three groups of charges versus $x/x^0 = 1/\cos \theta$ (x = thickness of air traversed; x^0 = thickness of air in the vertical direction). The statistical errors in the points are indicated.

The theoretical curves calculated from the diffusion equation are also plotted in the diagram. The full line corresponds to the values of the fragmentation

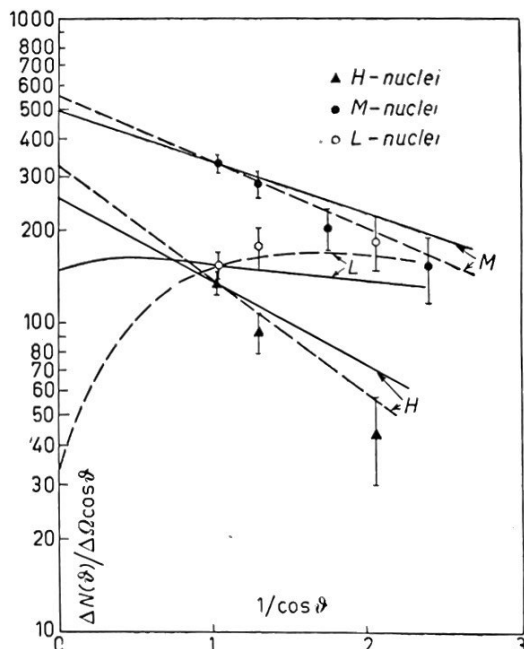


Fig. 5.

(*) In computing the solid angles $\Delta\Omega$ we took into account the fact that only tracks having an angle of dip $\leq 11^\circ 30'$ were accepted in this experiment.

probabilities of Table VI. The agreement is not bad, but an improvement could be reached (dashed curve) assuming for the fragmentation probabilities the values: $P_{LL} = 0.15$; $P_{ML} = 0.30$; $P_{MM} = 0.10$; $P_{HL} = 0.40$; $P_{HM} = 0.20$; $P_{HH} = 0.10$ that is for an increase in the P_{HL} and P_{ML} , and a reduction of the P_{MM} , P_{HH} , P_{HM} . This variation of the P_{IJ} ($I, J = L, M, H$) should be expected as a consequence, as we already pointed out in Sect. 8, of the inclusion in l -events of a 43% of peripheral collisions with heavy nuclei.

In spite of low statistics we report these results as a possible indication that the values of fragmentation probabilities deduced from the analysis of the interactions in the emulsion give only approximately the values in the atmosphere.

11. - Meson production.

In Tables III-*a* and III-*b* we have indicated with N_r all the relativistic prongs outgoing from the interaction, which could not be considered as splitting products. We now assume that N_r is the number of mesons produced in the interaction, neglecting the presence, between them, of some relativistic protons of the target nucleus. In order to estimate the variation of the meson production with energy and charge of the incoming nucleus, we proceeded as follows: we have tried to give a rough estimate of the average number \bar{N}_{N_p} of nucleon pairs interested in any single collision. In our estimate the simplifying hypothesis that $A = 2Z$ for all incident and target nuclei, was made.

It seems then reasonable to define in every collision:

$$N_{N_p} = Z_i + Z_t - Z_{z>1} - Z_{ev},$$

where: Z_i is the charge of the incoming nucleus; Z_t is the number of charged non-relativistic prongs outgoing from the interaction; $Z_{z>1}$ is the sum of the charges of the splitting products with $Z > 1$; Z_{ev} is the number of tracks of the target nucleus emitted with low energy ($I/I^0 > 4$) which could be considered as evaporation tracks.

We assume the average number of nucleon-nucleon collisions in every interaction to be equal to the number of above defined nucleon pairs. The average number \bar{N}_π of mesons produced in every nucleon-nucleon collision is then estimated.

In Table IX are reported the values of \bar{N}_π as a function of the energy and of the group of charge (L, M, H) of the incident nucleus for l -events and h -events. The data include all the interactions collected in Table III-*a* and III-*b*.

As mentioned in Sect. 16, the energy of the incoming nucleus was estimated in 242 cases (195 splitting of primaries and 47 splitting of secondaries) with

TABLE IX. — Energy dependence of meson production.

Energy (GeV per nucleon)	Charge group	<i>t</i> -events			<i>h</i> -events		
		No. of mesons in every collision	Total number of inter- actions	\bar{N}_{NP}	No. of mesons in every interaction	Total number of inter- actions	\bar{N}_{NP}
1.5— 4	L	1.7	23	3.3	0.49 ± 0.07	5.1	0.47 ± 0.15
	M	2.6	66	4.4	0.61 ± 0.05	7.3	0.64 ± 0.08
	H	2.7	23	7.3	0.36 ± 0.07	10.1	0.56 ± 0.08
1.5— 4	averaged value over <i>L, M, H</i>				0.52 ± 0.03		0.58 ± 0.04
	L	1.7	13	2.5	0.69 ± 0.15	10.0	4
	M	2.9	31	2.6	1.15 ± 0.15	14.7	8
4 — 10	H	3.1	15	5.7	0.54 ± 0.15	27.4	5
	averaged value over <i>L, M, H</i>				0.80 ± 0.08		
	L	1.3	8	1.9	0.7 ± 0.2	0	9.5
> 10	M	4.5	9	3.0	1.6 ± 0.3	12	1.1
	H	6.0	8	3.0	2.0 ± 0.5	36	1.8
	averaged value over <i>L, M, H</i>				1.5 ± 0.2		1.3 ± 0.2
> 10	L	1.3	8	1.9	0.7 ± 0.2	0	0
	M	4.5	9	3.0	1.6 ± 0.3	2	11
	H	6.0	8	3.0	2.0 ± 0.5	1	16
> 10							1.5 ± 0.7

methods independent from the number of relativistic particles outgoing from the interactions. In the remaining 89 cases this could not be done and an estimate of the energy was given by attributing to every relativistic track an energy of 1,0 GeV and correcting by a factor 2 for the neutral particles. In Table X we have compared the results of Table IX with those obtained excluding the 89 doubtful cases.

TABLE X. - *Check on meson production.*

Energy (Gev/nucleon)	Charge group	\bar{N}_π (<i>l</i> -events)		\bar{N}_π (<i>h</i> -events)	
		splitting	splitting and stars	splitting	splitting and stars
1.5-4	L	0.71 ± 0.15	0.49 ± 0.07	1.82 ± 0.08	0.47 ± 0.15
	M	0.48 ± 0.05	0.61 ± 0.05	0.75 ± 0.15	0.64 ± 0.08
	H	0.35 ± 0.06	0.36 ± 0.07	0.66 ± 0.14	0.56 ± 0.08
1.5-4	averaged value over L, M, H	0.45 ± 0.04	0.52 ± 0.03	0.71 ± 0.08	0.58 ± 0.04
4-10	L	0.68 ± 0.15	0.69 ± 0.15	1.1 ± 0.4	1.1 ± 0.4
	M	1.12 ± 0.15	1.15 ± 0.15	0.6 ± 0.3	1.1 ± 0.3
	H	0.56 ± 0.11	0.54 ± 0.15	1.1 ± 0.4	1.8 ± 0.6
4-10	averaged value over L, M, H	0.81 ± 0.08	0.80 ± 0.08	0.9 ± 0.2	1.3 ± 0.2
> 10	L	0.7 ± 0.2	0.7 ± 0.2		
	M	1.6 ± 0.4	1.6 ± 0.3		
	H	2.0 ± 0.5	2.0 ± 0.5		
> 10	averaged value over L, M, H	1.5 ± 0.2	1.5 ± 0.2	1.5 ± 0.7	1.5 ± 0.7

The comparison clearly indicates that adding these events we do not affect the results excepts obviously for an improvement of the statistics.

As it was to be expected, the average number of mesons produced in every so called nucleon-nucleon collision is roughly independent, within the limits of errors, from the group of charge of the incident nucleus and from the size of the target (*l*-events, *h*-events) and increases with the energy of the incoming nucleus. The value \bar{N}_π cannot be compared directly with the average number of mesons produced in free p-p or p-n collisions of the same energy but, if the

above given arguments are correct, should have the same dependence on the energy.

In Table IX, the average number \bar{N}_{np} of nucleon pairs for every collision is reported. Such a number decreases as the energy increases. This effect could have a physical meaning, but no conclusion can be drawn until Peters' relations used for the determination of the energy in most of the cases reported, are proved to be generally correct (cfr. Sect. 15).

12. - Ratio of even charged to odd charged secondaries.

It has been pointed out by GOTTSSTEIN (4) that, in the fragmentation of the heavy primaries, the probability of splitting into even charge fragments is greater for even charged primaries than for odd charged ones. In order to check this effect we collected our data in a diagram to be compared with the one given by GOTTSSTEIN. In Fig. 6 the ratio $N_{\text{even}}/N_{\text{odd}}$ of the number of secondaries of even charge to that of secondaries of odd charge (including protons) is plotted versus the charge Z of the primary nucleus. The figures in parenthesis represent the number of events on which the statistics is based. Only interactions in which the number of grey and black prongs is equal to or lower than seven (l -events) are taken into account.

As one sees, we find the same result as GOTTSSTEIN with a greater statistical weight. This seems to confirm the existence of the effect.

13. - Energy determination.

The determination of the energy of fast particles is a weak point in the emulsion technique, because all the methods which can be used are affected by errors whose magnitude is only very roughly established.

The energy of the tracks that do not interact in the emulsion can be determined only by scattering measurements. For energies certainly higher than 1 GeV, like the ones we have to study (the cut-off energy for this latitude was determined by FOWLER and WADDINGTON (9) to be 1.55 GeV per nucleon) one must use cell sizes of 1 mm or more and therefore only very flat tracks can be analysed. Consequently we decided to neglect the few measurable

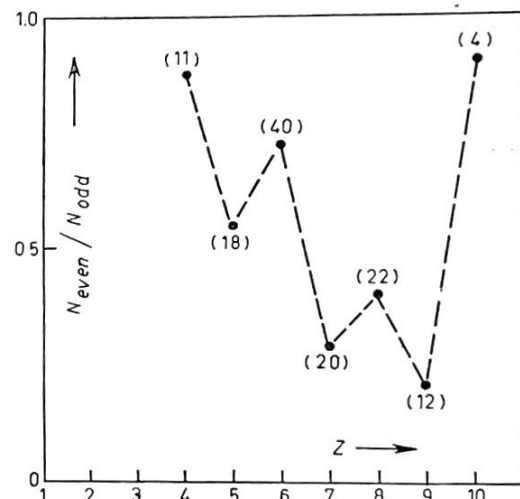


Fig. 6.

non-interacting tracks and to investigate the energy determination only on the interacting particles.

The measurements that one can make in order to determine the energy of an interacting heavy nucleus are the following:

- 1) For splitting events (where we assume that the energy of the primary and those of the splitting products are of the same order):
 - scattering on the primary and on the secondary tracks;
 - relative scattering on the splitting tracks;
 - angle of emission of the splitting tracks.
- 2) For star events:
 - scattering on the primary track;
 - number of black, grey and minimum prongs (from which the visible energy of the star can be derived ⁽⁴⁾).

14. - Scattering measurements.

Relative scattering measurements have been carried out with the usual method ⁽¹⁸⁾. They give very reliable results because they are not affected by spurious scattering and distortion of the plates. Unfortunately the measurements have to be confined to tracks fulfilling rather strict geometrical conditions: the distance between the two tracks must not exceed $50 \mu\text{m}$ in the y direction and $20 \mu\text{m}$ in the z direction (the direction of the primary defines the x -axis). This limitation results in a bias towards the tracks which, being emitted in a very narrow angle, are likely to be the most energetic ones.

Scattering measurements on individual tracks give reasonable results only if it is possible to eliminate the influence of spurious scattering. Since on the plates of stack Y the value of the spurious scattering has been already found to be small ⁽¹⁸⁾ and reliable results have been obtained for the energy of very fast protons, we felt justified in estimating the energy of the heavy primaries in the same stack with the same method. We selected for the measurements, tracks whose length per plate is greater than 2 cm and whose total path in the stack is longer than 5 cm. Moreover we compared the results with those obtained following the procedure proposed by FOWLER and WADDINGTON ⁽⁹⁾. The value of the mean sagittae obtained by the two methods are usually in good agreement within the statistical errors; the energy was derived by using the scattering constant ($K = 32$) proposed by the Bristol group ⁽⁹⁾.

⁽¹⁸⁾ A. DEBENEDETTI, C. M. GARELLI, L. TALLONE and M. VIGONE: *Nuovo Cimento*, **4**, 1142 (1956).

15. - Mean angle of emission of the α -particles.

The measurement of the angle of emission of the secondaries with respect to the direction of the primary, does not present any experimental difficulties and the error is usually small. We restrict ourselves to the study of the α -particles emitted in the splitting events because in the case of plateau ionization tracks it is impossible to distinguish between protons and created mesons.

The angle of emission of the α -secondaries in the laboratory system is related to the energy of the primary particle, but depends also from other factors (angle of emission and energy of the secondaries in the centre of mass system) that it is not possible to determine for each case. A very simple relation between the angle of emission and the primary energy has been given by PETERS (¹⁹) assuming that the α -particles are emitted isotropically and with a mean energy of 12 MeV in the centre of mass system. Peters' formula gives a result which is valid as a mean value, when the angles of many α -tracks are taken into account; but in the case of few tracks, as PETERS pointed out, this formula can easily give a large overestimate of the energy when the α -particles are emitted in the forward or backward direction in the centre of mass system. On the other hand, FOWLER *et al.* (¹²) observed that the mean angle of emission of the α -particles increases with increasing primary charge; using the integral energy spectrum proportional to $E^{-1.5}$ previously determined (⁹), they found that the mean energy of the α -particles in the centre of mass system increases with the primary charge and that in any case its value seems to be greater than 12 MeV. This effect would mean that the energy calculated with Peters' formula is underestimated.

Using our experimental data we looked for the effect of the primary charge on the mean angle of emission, and our results, collected in Table XI, are in perfect agreement with Fowler's ones (¹²).

TABLE XI. - Dependence of the mean angle of emission of α -particles from the charge of the primary.

Charge group	L	M	H
θ_α (degrees)	1.11 ± 0.12	1.35 ± 0.10	2.11 ± 0.19
No. of α -particles	49	115	69

(¹⁹) B. PETERS: *Progress in Cosmic Ray Physics*, Vol. 1, 193 (1952).

In the interpretation of the results we thought that the mean angle of emission of the secondary α -particles may not be a function of the charge of the primary, as it seems from the preceding table, but more likely a function of the number of nucleon pairs involved in the interaction. In order to prove if this assumption is correct, we divided the interactions in groups for which the number of nucleons is the same. This number has been determined for each event in Sect. 11 of the present work. For each group we calculated the mean angle of emission of the α -particles, and the results are given in Table XII.

TABLE XII. – *Dependence of the mean angle of emission of α -particles from the number of nucleon pairs interested in the collision.*

No. of nucleon pairs interested in the collision	0–1	2–3	4–5	6–7	≥ 8
θ_α (degrees)	0.92 ± 0.08	1.16 ± 0.12	1.66 ± 0.19	2.17 ± 0.38	2.46 ± 0.26
No. of α -particles	72	48	43	19	48

The increasing of the mean angle of emission of the α -particles when the number of nucleons involved in the collision increases, might be due to a corresponding increase of the mean energy of the α 's in the centre of mass system as suggested by FOWLER (12), or to some other effect. The energy of emission of the α -particles has been studied by some authors (20–22) but we do not know if their results can be applied to the stars produced by the heavy primaries. For this reason we think that it will be worthwhile to investigate this point using the interaction of the heavy primaries. Only after this analysis, that we plan to carry out in a next work, it will be possible to see if the number of nucleons involved in the interaction has to be accounted for in the determination of the energy.

16. - Energy spectrum.

On 275 interacting tracks measurements could be performed. In 80 events the energy of the primary was derived from the calculation of the visible energy of the star. In 195 splitting events, the energy was obtained from the angles of emission of the secondary nuclei by using Peters' formula.

(20) N. PAGE: *Proc. Phys. Soc., A* **63**, 250 (1950).

(21) D. H. PERKINS: *Phil. Mag.*, **41**, 138 (1950).

(22) G. BERNARDINI, G. CORTINI and A. MANFREDINI: *Phys. Rev.*, **79**, 952 (1950).

Moreover, in 69 out of the 195 splitting events, either scattering measurements or the study of secondary interactions gave independent values of the energy of the primary. Therefore the energy of these particles is better known, but we cannot base on them an investigation on the energy spectrum of the heavy particles, because, as we said before, the selection of tracks for relative scattering measurements introduces a bias towards the high energy region. Consequently we made use of these 69 tracks only to check if the statistical uncertainty introduced by Peters' formula has a great influence on a distribution of the tracks in wide energy intervals.

In Table XIII we compare the distribution obtained when we attribute to each track the energy evaluated from the angle of emission (distribution *A*), with the one obtained when the energy of the same tracks is estimated in an independent way (distribution *B*).

TABLE XIII. – *Check on energy distribution.*

Intervals of energy (GeV/nucleon)	$1.5 \leq E \leq 4$	$4 < E \leq 10$	$E > 10$
No. of tracks (distribution <i>A</i>)	36	24	9
No. of tracks (distribution <i>B</i>)	38	24	7

From the table one can see that if the tracks are divided in wide enough intervals of energy, the various independent methods of evaluating the energy give roughly the same number of tracks in each group. Therefore we think that an attempt to draw the slope of the energy spectrum of the primary particles can be reasonably made; using all the 275 tracks for which we have at least one estimate of the energy and distributing them in the same intervals of energy as in Table XIII we obtain the integral energy spectrum shown in Table XIV.

TABLE XIV. – *Integral energy spectrum.*

Energy (GeV/nucleon)	$E \geq 1.55$	$E > 4$	$E > 10$	$E > 50$
Number of tracks	275	91	26	2

Taking for the integral energy spectrum the expression:

$$N(E) = C(E + m_p c^2)^{-k},$$

(where $N(E)$ is the number of heavy primaries with an energy greater than E ; $(E + m_p c^2)$ is the total energy in GeV per nucleon, C and k are constants)

we find:

$$k = 1.54^{+0.16}_{-0.13}.$$

This value of the exponent k has been calculated under the assumption that the energy distribution does not depend on the charge of the primaries. Although we know that the statistics is very poor we did the same calculation for the primaries of charge $Z \geq 10$. We found for the exponent k the value: $1.5^{+0.3}_{-0.2}$ that seems to indicate that the above mentioned assumption is correct.

* * *

We wish to express our thanks to Prof. R. DEAGLIO and G. WATAGHIN for their constant interest and encouragement.

Thanks are due also to the President of the « Istituto Elettrotecnico Nazionale Galileo Ferraris » for the hospitality given in the photometric laboratory where charge measurements have been carried out with the valuable technical assistance of the photometric staff. We are greatly indebted to Prof. R. DEAGLIO for his helpful suggestions in the design of the photometric device.

The contribution of the scanner's team of our laboratory has to be acknowledged.

APPENDIX I

Comparison B-stack/Y-stack.

As the B and Y stacks have been exposed at the same latitude, the experimental data of the two stacks can be added to derive the energy spectrum and to increase the statistics in the analysis of interactions. On the contrary, to obtain the charge spectrum, we used only the results of the Y-stack. However, as the scanning in both stacks has been made under a nearly equal amount of matter ($\sim 16 \div 17 \text{ g/cm}^2$) the relative abundance of various elements obtained in the two experiments should not be very different except for Lithium and Berillium (owing to the bad scanning efficiency in the B-stack).

A comparison of the results seems therefore to be useful, on account of the good resolution obtained in ionization measurements, for the B-stack. The comparison is shown in Table XV in which the errors quoted are the statistical ones.

TABLE XV. – Comparison between B-stack and Y-stack.

	No. of B tracks	No. of B tracks	No. of C tracks	No. of N tracks	No. of O tracks	No. of H tracks
	No. of C tracks	No. of M tracks				
B-stack	0.59 ± 0.17	0.28 ± 0.07	0.52 ± 0.05	0.24 ± 0.02	0.13 ± 0.03	0.34 ± 0.08
Y-stack	0.47 ± 0.08	0.24 ± 0.04	0.51 ± 0.04	0.21 ± 0.02	0.17 ± 0.02	0.35 ± 0.04

APPENDIX II

Interactions with a nucleon target.

In Tables XVI (*a*, *b*) are given those interactions which can be interpreted as collisions with a single nucleon target (with no meson production). The

TABLE XVI-*a*. – *Interactions with a nucleon target in the Y-stack.*

Incoming nucleus	Target nucleon	Splitting	Charge identification
Li	n	$\alpha + p$	Photometric measurement
Li	n	$\alpha + p$	» »
Be	n	$\alpha + 2p$	C $\rightarrow \alpha + Be$; C: Photometric measurement and δ -ray counting; Be: δ -rays
Be	p (rel.)	2α	Gap counting
Be	n	$\alpha + 2p$	Photometric measurement
Be	n	$\alpha + 2p$	» »
B	n	$2\alpha + p$	Gap and δ -ray counting
B	p (rel.)	$2\alpha + p$	Photometric measurement and δ -rays
B	n	Be + p	Photometric measurement
B	p (rel.)	5p	» »
C	p (black)	3α	» »
C	n	2Li	C: splitting; Li: photometric measur.
C	n	3α	Photometric measurement
C	n	$2\alpha + 2p$	» »
C	n	Be + α	» » and gap counting
C	n	$2\alpha + 2p$	Photometric measurement
C	n	$2\alpha + 2p$	» »
C	n	3α	δ -ray counting
C	n	$2\alpha + 2p$	Photometric measurement
C	n	Li + 3p	C: Photom. measur.; Li: photom. measur.
N	n	B + α	N: δ -ray and gap counting
N	n	$3\alpha + p$	B: δ -rays and photometric measurement
N	n	Be + $\alpha + p$	Photometric measurement
N	p (rel.)	B + α	N: Photom. measur.; Be: gap counting
N	p (rel.)	$\alpha + 5p$	N: δ -rays; B: photometric measurement
N	p (black)	$\alpha + 5p$	Photometric measurement
O	n	4α	» »
O	n	C + α	O: splitting; C.: Photometric measurement
O	p (grey)	N + p	O: Photom. measur.; N: Photom. measur.
F	n	N + α	F: splitting; N: δ -rays
F	n	N + α	F: Photom. measur.; N: Photom. measur.
Ne	n	C + 2α	Ne: δ -rays; C: Photometric measurement
Na	n	F + α	Na: δ -rays; F: δ -rays

collisions with a single proton target include collisions either with a free proton in the emulsion or with a bound proton of the emulsion nuclei.

We tried to estimate the cross-section of the heavy incoming nuclei with a proton target in emulsion and to compare our results with the experimental cross-section obtained by exposing a heavy nucleus target to a 860 MeV proton beam (¹⁷). In order to do this, we must also take into account the interactions which can be interpreted as collisions with a proton target where some mesons were produced. Such events can not be positively identified and we

TABLE XVI-b. - *Interactions with a nucleon target in the B-stack.*

Incoming nucleus	Nucleon target	Splitting	Charge identification				
Be	p (black)	2α	Photometric measur. and δ -ray counting				
B	n	$2\alpha + p$	»	»	»	»	»
B	p (rel.)	$2\alpha + p$	»	»	»	»	»
B	p (grey)	$2\alpha + p$	»	»	»	»	»
C	n	3α	»	»	»	»	»
C	p (black)	$2\alpha + 2p$	»	»	»	»	»
C	n	$Be + \alpha$	C: Photometric measurement and δ -rays Be: » » » » »				
O	p (black)	$N + p$	O: Photometric measurement and δ -rays				
			N:	»	»	»	»
F	n	$N + \alpha$	F:	»	»	»	»
			N:	»	»	»	»
F	n	$N + \alpha$	F:	»	»	»	»
			N:	»	»	»	»

can only set an upper limit to their number. This was done by selecting all the events in which the number of outgoing charges exceeded the charge of the incoming nucleus and where at most one non-realistivistic track was noticed. In order to avoid errors due to some imprecision in the determination of charge we restricted our analysis to incoming charges $3 \leq Z \leq 10$.

The values of the total cross-section (with and without meson production) of heavy nuclei with a proton target emulsion is reported in Table XVII.

TABLE XVII. - *Collision with proton target in emulsion ($3 \leq Z_i \leq 10$).*

	No. of collisions with no meson production	Max. number of collisions with meson production	Total range (cm)	σ_H (cm · 10^{-25}) elastic (no mesons)	σ_H (cm · 10^{-25}) total (max. value)	σ_p (cm · 10^{-25}) experimental value of CHEN (¹⁷)
Y+B stack	16^{+2}_{-3}	22	3752	1.5 ± 0.6	3.5 ± 0.5	2.1

This value compared with the correspondent one obtained in (17) shows that at most 40% of the collisions with a proton target in emulsion occurs with a bound proton of an emulsion nucleus. This results is in good agreement with what found independently by other authors (23).

(23) R. CESTER, T. F. HOANG and A. KERNAN: *Phys. Rev.*, **103**, 1443 (1956).

RIASSUNTO

Sono state analizzate 529 tracce di nuclei pesanti, primari della radiazione cosmica. Su tutte le tracce sono state eseguite misure di carica utilizzando un dispositivo fotometrico; per controllo si sono eseguite misure di carica con conteggio di gap su tracce di boro e carbonio. Tutte le tracce sono state seguite nell'emulsione; nel corso delle osservazioni sono state rilevate 331 interazioni nucleari. L'analisi di queste interazioni ha permesso di determinare il libero cammino medio e le probabilità di frammentazione in emulsione ed in aria. I risultati, che sono in buon accordo con quelli ottenuti in altri laboratori, sono stati utilizzati per estrapolare al top dell'atmosfera lo spettro di carica. Al top dell'atmosfera il valore del rapporto tra nuclei leggeri e nuclei medi è 0.30 ± 0.09 , quello del rapporto tra nuclei pesanti e nuclei medi è 0.51 ± 0.11 . È stata misurata l'energia di 275 tracce per determinare l'esponente K che compare nella formula $N(E) = C(E + m_p C^2)^{-K}$ dello spettro integrale. Il risultato è $K = 1.54^{+0.16}_{-0.13}$. L'analisi è stata eseguita utilizzando la relazione di Peters tra l'energia del primario e l'angolo di emissione dei prodotti di frammentazione. I limiti di validità di tale relazione sono discussi nel corso del lavoro.